Catalytic Oxidation of Elemental Mercury over the Modified Catalyst Mn/α-Al_2O_3 at Lower Temperatures

JIANFENG LI, NAIQIANG YAN,* ZAN QU, SHAOHUA QIAO, SHIJIAN YANG, YONGFU GUO, PING LIU, AND JINPING JIA

School of Environmental Science and Engineering, Shanghai Jiao Tong University, Shanghai 200240, China

Received July 15, 2009. Revised manuscript received November 7, 2009. Accepted November 9, 2009.

In order to facilitate the removal of elemental mercury (Hg^0) from coal-fired flue gas, catalytic oxidation of Hg^0 with manganese oxides supported on inert alumina (α-Al_2O_3) was investigated at lower temperatures (373−473 K). To improve the catalytic activity and the sulfur-tolerance of the catalysts at lower temperatures, several metal elements were employed as dopants to modify the catalyst of Mn/α-Al_2O_3. The best performance among the tested elements was achieved with molybdenum (Mo) as the dopant in the catalysts. It can work even better than the noble metal catalyst Pd/α-Al_2O_3. Additionally, the Mo doped catalyst displayed excellent sulfur-tolerance performance at lower temperatures, and the catalytic oxidation efficiency for Mo(0.03)−Mn/α-Al_2O_3 was over 95% in the presence of 500 ppm SO_2 versus only about 48% for the unmodified catalyst. The apparent catalytic reaction rate constant increased by approximately 5.5 times at 423 K. In addition, the possible mechanisms involved in Hg^0 oxidation and the reaction with the Mo modified catalyst have been discussed.

Introduction

Mercury emitted from coal-fired power plants has become a major environmental issue because of its volatility, persistence, and bioaccumulation (*1, 2*). An agreement to launch United Nations Environment Programme (UNEP) Mercury Treaty Negotiations have been approved at UNEP's 25th GC Session in 2009 (*3*). Worldwide, China is regarded as one of the larger emitters of mercury, and coal-fired utilities are believed to be the largest anthropogenic sources in China (*4*−*6*).

Mercury in coal combustion flue gas includes three forms: elemental mercury (Hg^0), oxidized mercury (Hg^{2+}), and particulate-bounded mercury (Hg^p) (*7, 8*). Hg^{2+} is water-soluble and therefore might be effectively captured by wet flue gas desulfurization (FGD) systems as a cobenefit (*6*−*10*). Most Hg^p can be collected by electrostatic precipitators (ESPs) or fabric filters together with fly ash. However, Hg^0 is the most difficult to be removed because of its high volatility and low solubility in water. The conversion of Hg^0 to its oxidized form can thus facilitate its capture from the flue gas. It has been reported that some catalysts used for the selective catalytic reduction of nitric oxides (SCR) were able to improve the oxidation of Hg^0 to Hg^{2+} as an additional benefit when enough HCl was present in the flue gas (*10*−*16*). In order to develop the task-specific catalysts or sorbents for Hg^0 removal, some noble metals or transition metal oxides were also investigated for such a purpose (*13*). Noble metal catalysts, such as gold (Au) and palladium (Pd), have been shown to assist the catalytic oxidation of Hg^0 at lower temperatures, but they are considered too expensive for industrial applications. It has been found that manganese oxides on some carriers (e.g., titania or Al_2O_3) displayed significant catalysis for Hg^0 oxidation at higher temperatures (*10, 11*). To meet such temperature demands, the catalyst unit must be installed upstream of the air preheater and the particulate control devices. This location may result in catalyst deactivation by exposure to high concentration of fly ash. The effect of fly ash can be minimized if the catalysts can be located downstream of the particulate control devices, where the temperature of the flue gas is relatively low. Therefore, developing higher activity catalysts operating at lower temperatures (373−523 K) has been of the great interest. Recently, the authors have investigated the performance of the catalysts of manganese oxides (*11*). It was found that the catalysts were less active at lower temperatures and that SO_2 had a significant negative effect on their performance. To improve their performance at lower temperatures, modification of the catalysts with several metal elements was investigated, and the catalysts were characterized by various techniques.

Experimental Section

Materials. It was found in our previous study that the catalysts with porous γ−Al_2O_3 as the carrier displayed very large adsorption capacity with Hg^0 (*11*). The adsorption duration was very long, which would interfere with the test results for the net catalytic activity. In order to minimize this adsorption, inert alumina (α-Al_2O_3) pellets were used as the carrier in this study. The carrier consisted of pellets with a diameter of 1.5 ± 0.5 mm, and the BET surface area was 0.40 m^2/g. All chemicals used for the catalysts preparation were of analytical grades, and purchased from Sigma-Aldrich Co. and Sino-pharm Chemical Reagent Co. Gases of SO_2 (100%), NO(100%) and HCl (5000 ppm) were produced by Dalian Special Gas Co. The original gases were diluted to 200−1000 ppm by nitrogen, and then were added to the simulated gas through the mass flow controllers (MFCs). Compressed air and nitrogen in gas cylinders were used for the balance of the gases to prepare the simulated flue gases.

Catalysts Preparation. The manganese based catalysts were all prepared by the wet impregnation methods as follows. The aqueous solution of $Mn(NO_3)_2$ and the doped metal precursors, e.g., $Sr(NO_3)_2$, $Na_2WO_4 \cdot 2H_2O$, $Cu(NO_3)_2$, and $(NH_4)_6Mo_7O_{24} \cdot 4H_2O$ were dissolved in deionized water at the room temperature, then the dried α-Al_2O_3 pellets were added to the solutions. After impregnation for 2 hours (h), the pellets were dried at 333 K for 12 h; then followed by calcination in air at 573 K for 1 h and at 673 K for 3 h. The doped catalysts were expressed as M(*y*)−Mn/α-Al_2O_3, in which M represents the added metals, and *y* represents the mole ratio of the added metal to Mn, the weight percentage of the impregnated Mn to α-Al_2O_3 was set at 1% in this study if it was not stated clearly. In order to evaluate the effect of the modified catalysts, the noble metal catalyst Pd(1%)/α-Al_2O_3 was used for comparison, it was prepared by the same method as Mn(1%)/α-Al_2O_3.

Catalytic Activity Evaluation. The catalytic activity was evaluated in a fixed-bed reactor, which was similar to that in our previous study (*11*). The reactor (i.d., 6 mm) consisted

* Corresponding author phone: +86 21 54745591; fax: +86 21 54745591; e-mail: nqyan@sjtu.edu.cn.

10.1021/es9021206
Published on Web 12/01/2009

of two quartz tubes: one was filled with 1.25 g of the catalysts, and the other contained the same amount of α-Al_2O_3 without any catalysts, as the reference. The simulated flue gases compositions were prepared in situ. The inlet flow rate of each gas stream was accurately controlled by MFCs. Hg^0 vapor was prepared from the Hg^0 permeation unit (placed in an oil bath with a temperature of 333 K) and was blended with the gases before they entered the reactor. Hg^0 in the effluent stream was continuously monitored with an online mercury analyzers, and the data was recorded with a data acquisition system (N-2000). The reactions were mainly performed under atmospheric pressure at 373−523 K which was controlled by a tubular-furnace. The total flow rate was 50 L/h and a space velocity (SV) of $4.4 \times 10^4\ h^{-1}$ was obtained. The tests consisted of the adsorption and catalytic oxidation processes. The catalyst was first exposed to the simulated flue gas for hours or days, until the Hg^0 breakthrough in the outlet gas reached at least 80% of inlet Hg^0 concentration. This was followed by the tests on catalytic activity in the presence of HCl.

A cold vapor atomic absorption spectrophotometry analyzer (SG921, Jiangfen, China) was used as the continuous emission monitor to measure Hg^0 concentration continuously. The Ontario Hydro Method (OHM) was used to test the balance of mercury before and after the conversion. The OHM samples analysis and the adsorbed mercury on the catalysts were determined by a RA-915$^+$ mercury analyzer (Lumex, Russia) equipped with a liquid analysis unit and a solid pyrolysis unit (RP-91C), respectively.

Characterization of the Catalysts. To determine the crystals species distribution in the catalyst, X-ray diffraction (XRD) measurements were carried out with a diffractometer (D/max-2200/PC, Rigaku, Japan) using Cu Kα radiation. X-ray photoelectron spectroscopy (XPS, PHI-5000C ESCA) measurements were used to determine the Mn $2p^3$ and O 1 s binding energies with Mg Kα radiation ($h\nu = 1253.6$ eV). The C1s line at 284.6 eV was taken as a reference for the binding energy calibration. Transmission electron microscopy (TEM) was used to investigate microstructures of the catalysts with an electron microscope (JEM-2010, JEOL, Japan) and the selected area electron diffraction (SAED) patterns were obtained at the same time. Hydrogen temperature program reduction (H_2-TPR) experiments were carried out on a CHEMBET 3000 (Quantachrome, U.S.) by increasing the temperature from 60 to 700 °C at a rate of 10 °C/min. The specific surface area of the catalysts was tested using Brunauer−Emmett−Teller (BET) method (ASAP 2010, Micromeritics Inc., U.S.).

Results and Discussion

Performance of Mn/α-Al_2O_3 at Lower Temperatures. As shown in Figure 1, the increasing of the adsorption temperature from 423 to 523 K was unfavorable for the adsorption of Hg^0. The half breakthrough time of Hg^0 dropped from about 240 min at 423 K to 35 min at 523 K in the absence of SO_2. This result was different from our previous tests on the catalysts with γ−Al_2O_3 as the carrier (*11*). Additionally, the effect of SO_2 on adsorption was remarkable, especially for the adsorption at lower temperatures. The presence of 500 ppm SO_2 in the flue gas resulted in the reduction of the half breakthrough time to 30 and 18 min at 423 K and 523 K, respectively. The results indicated that the presence of SO_2 could inhibit the adsorption of Hg^0 onto the catalyst especially at lower temperatures.

Once the Hg^0 adsorption breakthrough efficiency was over 80%, HCl was continuously injected into the gas to investigate the performance of catalytic oxidation of Hg^0 over various catalysts. These results are also shown in Figure 1(b). It was obvious that the presence of HCl enhanced the removal of Hg^0. It was also observed that the removal of Hg^0 by catalytic oxidation with 20 ppm HCl at 423 K (73%) was lower than

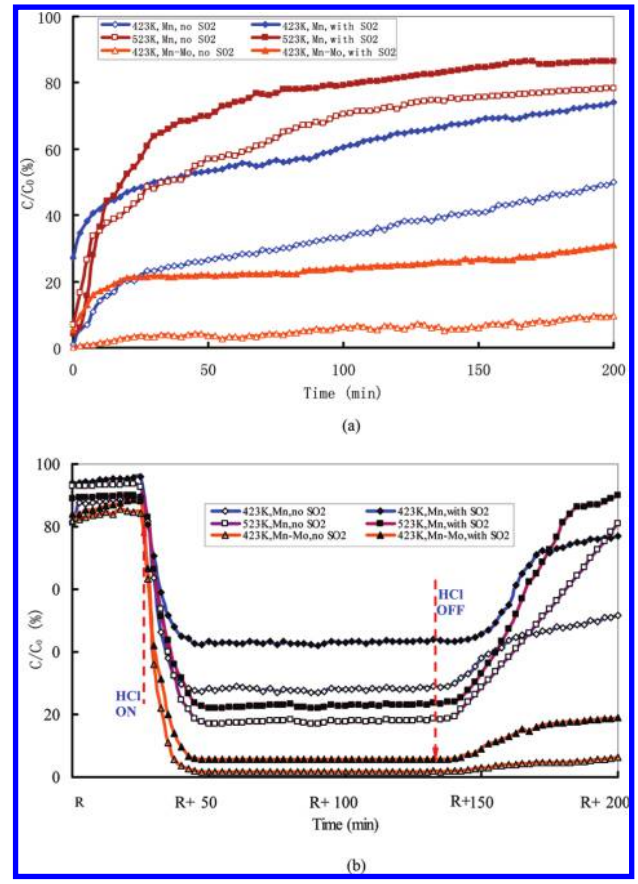

FIGURE 1. Breakthrough curves of elemental mercury by adsorption and catalytic oxidation. (a) Adsorption in the absence of HCl; (b) Adsorption and catalytic oxidation with 20 ppm HCl. The space velocity was 44000 h^{-1} and the inlet Hg^0 concentration in the gas, C_0, was about 20ppbv. It was 500 ppm for SO_2 if it was used.

that at 523 K (84%), and the catalyst Mn/α-Al_2O_3 was less active below 523 K. The balance of mercury with OHM indicated that almost all the removed Hg^0 in the presence of HCl was converted to oxidized mercury, with the balance of 95(±10)% for the total mercury between in the inlet gas (Hg^0) and the outlet (Hg^{2+} and Hg^0). The presence of SO_2 also showed a significant inhibition to Hg^0 catalytic conversion at lower temperatures.

Temperature Dependence of the Catalysts with Various Doping Elements. Since Mn/α-Al_2O_3 catalyst was less active for Hg^0 conversion at lower temperatures or in the presence of SO_2, several metal elements (Sr, W, Cu, and Mo) were tentatively doped into Mn/α-Al_2O_3 to improve the performance of the catalysts, and Pd(1%)/α-Al_2O_3 catalyst was employed as a reference as well.

The adsorption and catalytic behavior for Mo−Mn/α-Al_2O_3 is also illustrated in Figure 1. As can be seen, the adsorption and the catalytic performance at lower temperatures were both significantly improved by the addition of Mo. The half breakthrough time for Hg^0 adsorption in the absence of SO_2 increased to about 2000 min versus about 240 min for the Mn/α-Al_2O_3 catalyst at 423 K. However, The Hg^0 half breakthough for sole Mo/α-Al_2O_3 was only 120 min.

The catalytic oxidation efficiency of Hg^0 by Mo(0.01)−Mn/α-Al_2O_3 with 20 ppm HCl (without SO_2) was about 95% at 423 K, with an increase of about 20% over Mn/α-Al_2O_3(as the baseline). Furthermore, the Hg^0 oxidation efficiencies for the catalysts with other doping elements at different temperature are shown in Figure 2 (with 10 ppm HCl). It was seen that the doping of other elements into Mn/α-Al_2O_3 could also improve the catalytic activity at lower temperatures. Mo was

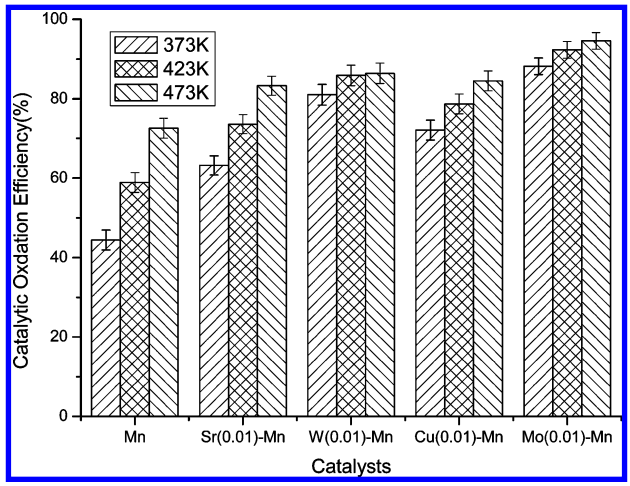

FIGURE 2. Temperature dependence of Hg^0 catalytic oxidation efficiencies for various doped catalysts with 10 ppm HCl (in the absence of SO_2).

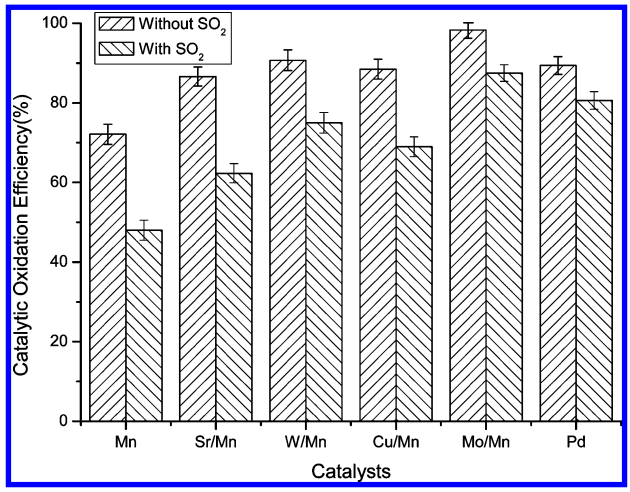

FIGURE 3. Comparison of the Hg^0 catalytic oxidation efficiencies with and without SO_2 for the various doped catalysts at 423 K (20 ppm HCl).

found to be the best among the tested dopants, and the addition Mo (0.01) to the catalyst can decrease the operation temperature by at least 80 K while still achieving the same Hg^0 oxidation efficiency (Figure 3). By comparison, Mo(0.01)−Mn/α-Al_2O_3 showed higher Hg^0 catalytic oxidation efficiency than Pd/α-Al_2O_3 under similar conditions. However, the Hg^0 oxidation efficiency on sole Mo(1%)/α-Al_2O_3 at 423 K was about 30% with 20 ppm HCl. Therefore, Mo just acted as the promoter in Mn/α-Al_2O_3 because the catalysis of its sole was rather low. In addition, the effect of NO (0−400 ppm) on the catalysts was observed to be insignificant.

The Effect of SO_2 on Various Catalysts. Manganese based materials have been found to be able to adsorb sulfur dioxide at lower temperature (*17*), which might deteriorate the catalyst's performancefor Hg0 conversion. The activity of each catalyst was investigated in the simulated flue gas with 500 ppm SO_2. For the adsorption, the addition of Mo and W can increase the $t_{1/2}$ obviously. The $t_{1/2}$ for Mn/α-Al_2O_3 in the presence of SO_2 at 423 K was only about 30 min, but it was more than 350 min when Mo(0.01) was doped into the Mn/α-Al_2O_3 catalyst.

The effects of SO_2 on the Hg^0 oxidation with various catalysts are shown in Figure 3. As can be seen, the inhibition effect of SO_2 varied for different catalysts. The Hg^0 oxidation efficiency of Mn/α-Al_2O_3 with 20 ppm HCl dropped from 93 to 78% (in Figure 1), a loss of about 15% at 573 K in the presence of SO_2. However it sharply decreased from about

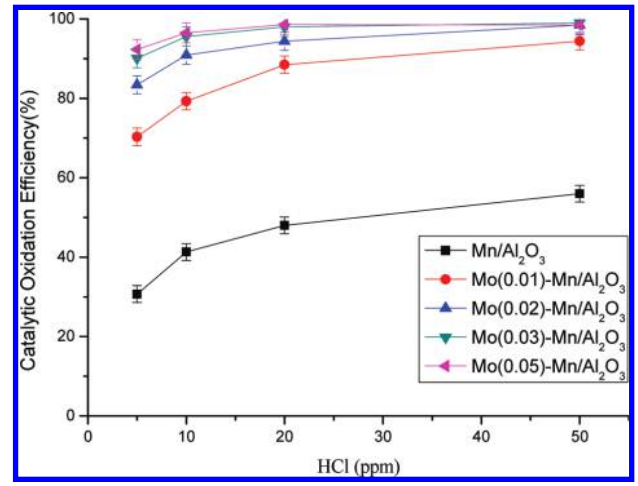

FIGURE 4. The effect of the doped Mo content on the Hg^0 oxidation efficiency at various HCl concentrations and at 423 K (with 500 ppm SO_2).

73 to 48% at 423 K, with a loss of 25%. This indicated that the inhibition of SO_2 on the activity of Mn/α-Al_2O_3 was more remarkable at lower temperatures. Among the modified catalysts, Mo(0.01)−Mn/α-Al_2O_3 showed the best resistance to the inhibition of SO_2, Hg^0 oxidation efficiency decreased from about 95 to 88% (7% loss) at 423 K in the presence of 500 ppm SO_2. Doping Sr into Mn/α-Al_2O_3 can also improve its catalytic activity at lower temperatures, but its performance against the inhibition of SO_2 was relatively weak. Mo(0.01)−Mn/α-Al_2O_3 also showed higher tolerance to SO_2 than Pd/α-Al_2O_3, which was only about 80% at 423 K in the presence of 500 ppm SO_2.

Additional tests were performed to determine the possible reasons that SO_2 influenced on catalysts' activities. First, the Mn/α-Al_2O_3 catalyst was continuously pretreated with 500 ppm SO_2 (dry air as the balance) at 423 K for 10 h before their catalytic activity tests. It was found the Hg^0 conversion efficiency decreased by about 16% comparing with the untreated fresh catalyst in the absence of SO_2, and further dropped to about 26% in the presence of 500 ppm SO_2. Meanwhile, the effect of SO_2 on the Hg^0 adsorption on Mn/α-Al_2O_3 was more remarkable, and Hg^0 adsorption capacity would loss over 80% in the coexistence of 500 ppm SO_2. The above results indicated that SO_2 could cause a permanent activity loss maybe by the combination with catalyst elements. And a possible temporary and reversible effect maybe resulted in the competitive adsorption between SO_2 and Hg^0 on the catalyst's active sites, which has ever been proposed in the similar study (*14*). Therefore, it can been regarded that the doped Mo in catalysts might be helpful to diminish the competitive adsorption of SO_2 with Hg^0 or the permanent coverage by SO_2 on Mn-base active sites because the larger affinity of Mo to sulfur would minimize the chance of the contact of sulfur and Mn (*18*−*20*). However, further investigations are required to support the hypothesis.

Effect of the Doped Content Mo and HCl Concentration. The effect of the doped content of Mo into the catalysts was also investigated and the results are shown in Figure 4. As expected, the catalytic oxidation efficiency of Hg^0 increased with the increase of the doped amount of Mo. Hg^0 oxidation efficiency at 423 K with 20 ppm HCl in the presence of 500 ppm SO_2 was only 48% for the Mn/α-Al_2O_3 without Mo addition, but it was about 87% and 95% when the doped mole ratios of Mo to Mn were 0.01 and 0.03, respectively. The enhancement effect tended to be flat as the doped mole ratios of Mo to Mn exceeded 0.03.

Meanwhile, the effect of HCl concentration on the Hg^0 oxidation efficiency is also shown in Figure 4. Higher HCl concentration was favorable for the catalytic oxidation of

TABLE 1. Kinetics Parameters for Various Catalysts[a]

catalysts	temperature (K)	SO_2	β	εK_s (mg/m^{3}s)	constant ratio[c]
Mn/α-Al_2O_3 (baseline)	423	W/o[b]	0.37 ± 0.02	4.2 ± 0.3	1
Mo(0.01)−Mn/α-Al_2O_3	423	W/o	0.36 ± 0.02	11.4 ± 0.5	2.6
Mn/α-Al_2O_3	423	W	0.37 ± 0.02	2.1 ± 0.2	1
Mo(0.01)−Mn/α-Al_2O_3	423	W	0.36 ± 0.02	6.5 ± 0.5	3.0
Mo(0.03)−Mn/α-Al_2O_3	423	W	0.36 ± 0.02	11.7 ± 0.5	5.5
Mo(0.01)−Mn/α-Al_2O_3	373	W	0.36 ± 0.02	5.4 ± 0.5	
Mo(0.01)−Mn/α-Al_2O_3	473	W	0.36 ± 0.02	7.2 ± 0.5	

[b] W/o: in the absence of SO_2 in the gas; W: with 500 ppm SO2 in the gas [c] The ratio of the apparent catalytic reaction rate constant to the baseline. [a] Mn: Mn/α-Al_2O_3.

Hg^0. The required HCl concentration was lower using the modified catalysts with the higher Mo amount. Only 5 ppm of HCl was needed to obtain 90% Hg^0 oxidation efficiency when the doped mole ratios of Mo to Mn was about 0.03. Additionally, since $\gamma-Al_2O_3$ was more porous than α-Al_2O_3, a better performance was expected if $\gamma-Al_2O_3$ was employed as the catalyst carrier.

Kinetics for the Typical Catalytic Reaction. Equation 1 is tentatively used to express the rate of Hg^0 catalytic oxidation.

$$r_A = K_s[HCl]^{\beta}[Hg^0] \quad (1)$$

in which, r_A is the specific reaction rate for Hg^0 oxidation on the catalyst, mg/(m^2·s), K_s is the apparent catalytic reaction rate constant, m/s., and β is the reaction order with regard to HCl concentration, dimensionless. Since the employed HCl concentration in the reactor was far higher than Hg^0 and the consumed HCl was almost negligible, HCl concentration could be regarded as a constant (*21*, *22*). Therefore, eq 2 can be obtained with eq 1.

$$[Hg^0]/[Hg^0]_0 = \exp\{-K_s\varepsilon[HCl]^{\beta}t\} \quad (2)$$

Where ε is the specific area per unit volume of the catalyst, m^2/m^3. The relationship of $\ln\{-\ln([Hg^0]/[Hg^0]_0)\}\sim[HCl]$ should be linear if eq 1 was suitable for the description of the kinetics. As expected, it was observed that the $\ln\{-\ln([Hg^0]/[Hg^0]_0)\}\sim[HCl]$ curves for the tested catalysts showed linear performance, which indicated that the catalytic reaction rate conformed to the pseudo first order with respect to Hg^0. Then β and $K_s\varepsilon$ in eq 2 can be obtained by graphing with the data obtained by graphing with the data obtained above, and the main results are listed in Table 1. It can be seen that the values of β for various catalysts were very close to one other (0.36 ± 0.02), but the value of K_s varied significantly. The enhanced factor, defined as the K_s ratio of the doped catalyst to the unmodified (baseline), can also be employed to assess the performance of the catalyst, and it was about 5.5 for the catalyst of Mo(0.03)−Mn/α-Al_2O_3 at 423 K in the presence of 500 ppm SO_2.

Characterization of the Catalysts. The BET area were determined to be about 0.57 m^2/g, 0.87 m^2/g, 1.10 m^2/g, and 1.18 m^2/g for the sloe Mn/Al_2O_3, Mo(0.01)−Mn/Al_2O_3, Mo(0.03)−Mn/Al_2O_3 and Mo(0.05)−Mn/Al_2O_3, respectively. Both of them slightly decreased after 24 h tests (by about 5−10%). The XRD patterns of the catalysts with α-Al_2O_3 as the carrier appeared too weak to identify the crystals of Mn or Mo on the catalysts because of lower load content (<2%). In order to explain the effect of Mo on the Mn/α-Al_2O_3 catalyst more clearly, powdered $\gamma-Al_2O_3$ was used as the catalyst carrier to obtain a higher load content of Mn and Mo in the catalyst. Figure 5 shows XRD patterns of (20%)Mn/Al_2O_3 and Mo(0.15)−Mn(20%)/Al_2O_3. It can be seen that Mn mainly presented in the form of MnO_2, and the peak for Mn_2O_3 can also been observed. The Mo in the doped catalyst was mainly found as MoO_3. It was found that the full width at half maximum (fwhm) of MnO_2 and Mn_2O_3 peaks slightly increased after doping with Mo. The higher XRD fwhm of the crystalline indicated the smaller size of the particles, which indicated that Mo can improve the dispersion of MnO_x particles by inhibiting the agglomeration.

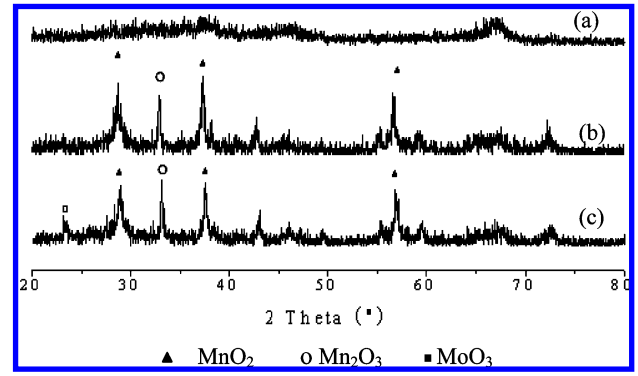

FIGURE 5. The XRD patterns for (a)Al_2O_3, (b) Mn/Al_2O_3, and (c) Mo(0.15)−Mn/Al_2O_3.

It was also observed from the TEM micrograph of Mn/Al_2O_3 (Figure 6) that the particles were not well dispersed. However, for the Mo−Mn/Al_2O_3 catalyst, the observed particles appeared to be smaller. Also, the SAED patterns of the two catalysts (at the right down corner of TEM pictures) also showed the Mn/Al_2O_3 appeared to be the single crystal diffraction spots and the Mo/Mn/Al_2O_3 had the poly crystal diffraction rings within the same scanned surface area. This indicated that the crystalline of Mn catalyst was larger than the Mo doped one. The result agrees well with the XRD fwhm results.

Figure 7 shows the temperature program reduction (TPR) curves of the catalysts by hydrogen. It was shown that the addition of Mo to the catalyst resulted in the flattening of the TPR curves. The reduction startup temperature decreased to about 423 K, though the peak was relatively low. Meanwhile, the main TPR curves of the modified catalyst shifted to a higher temperature. Although the lower TPR reduction startup temperature can be used to explain why the catalyst showed better catalytic activity at lower temperatures, it should not be the only factor considered to interpret such remarkable results for Hg^0 conversion. Meanwhile, the shift of TPR curves might implicate that Mo−Mn complex was formed on the catalysts, which would result in a better tolerance to SO_2 (*18*−*20*). The XPS analysis results for Mn2p (Figure 8) indicated that doping Mo into the catalysts can increase the ratio of Mn^{4+}/Mn^{3+}, which was favorable for the reaction with Hg^0, and this effect of the change were consistent with the Deacon process described below. The increase of binding energy of O1s may implicate that the ratio of lattice oxygen (O^{2-}) to other oxygen species (e.g. oxygen in O_2^{2-} or hydroxide) dropped when Mo was doped in the catalysts.

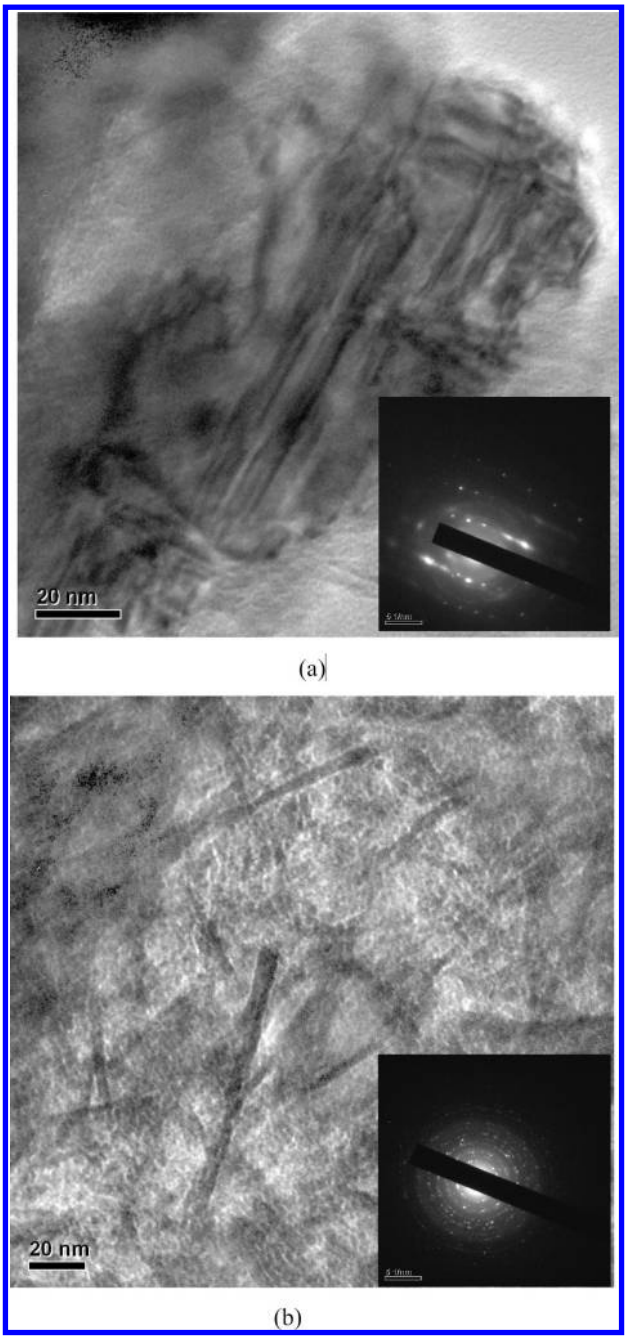

FIGURE 6. The TEM micrographs and the SAED patterns of the catalysts: (a) Mn/Al_2O_3 and (b)$Mo(0.15)-Mn/Al_2O_3$. Note: the SAED patterns were at the right down corner of TEM pictures.

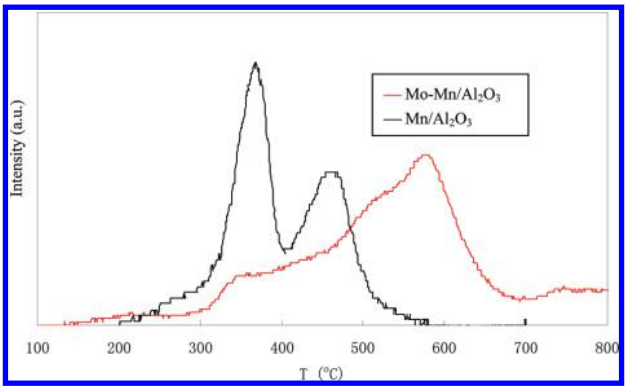

FIGURE 7. The TPR profiles for Mn/Al_2O_3 and $Mo(0.01)-Mn/Al_2O_3$ catalysts.

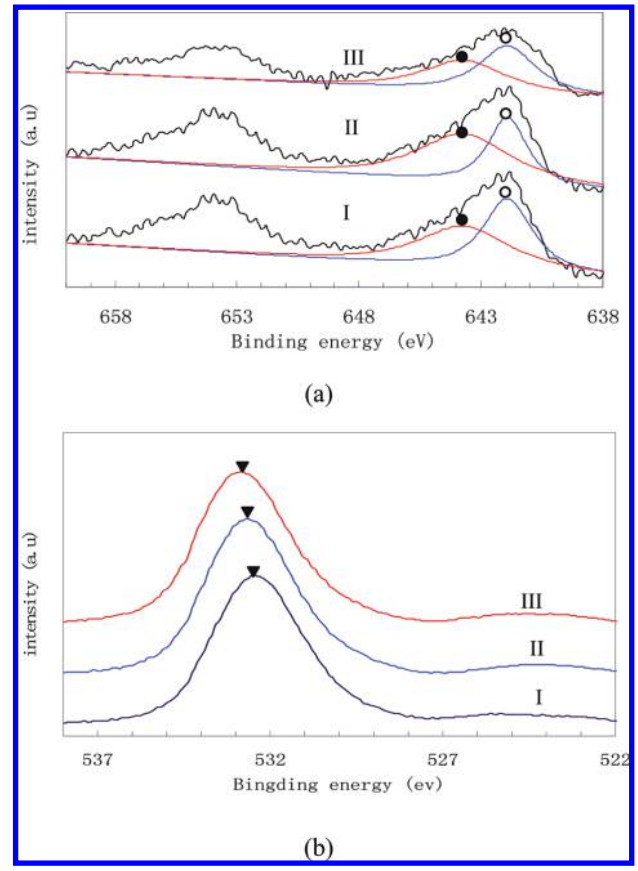

FIGURE 8. The XPS spectra for (a) Mn2p and (b) O1s of the catalysts: (I) Mn/Al_2O_3, (II) $Mo(0.01)-Mn/Al_2O_3$, and (III) $Mo(0.01)-Mn/Al_2O_3$ with adsorbed Hg. ● Mn^{4+}; ○ Mn^{3+}; ▼ O1s.

Speculation on the Mechanism for the Modified Catalysts. From the tests results of the catalysts, the low-temperature catalytic activity and the ability to tolerate poisoning from sulfur dioxide can be remarkably improved by the doping of Mo oxide. According to our preliminary tests, Cl_2 was apparently detectable when it was over 573 K, and the yield of Cl_2 with Mo doped catalyst was about 50% higher than Mn catalyst at the similar test condition. Therefore, the doping of Mo in the catalyst was proved to be favorable to the Deacon reaction (*22*). In addition, the shift of the main TPR curves to higher temperature may indicate that more stable compound formed after Mo was doped. Thus based on the above experimental results, the mechanism for the functions of Mo in the catalyst can be speculated as follows: First, the impregnated manganese precursor on the Al_2O_3 carrier would be converted to particles of manganese oxides as the catalyst was calcined. These particles would tend to agglomerate and then form crystalline Mn oxides during the sintering process. The crystalline Mn oxides were unfavorable for the catalytic activity and the sulfur tolerance. The doped Mo in the catalysts could partly form Mo oxides among the particles of Mn oxides or Mo−Mn compound and the agglomeration of particles would be effectively inhibited. In addition, the presence of Mo−Mn complex was supposed to improve the sulfur resistance performance (*18*−*20*). These might promote the Deacon reaction to form reactive chlorine species (e.g., Cl_2 or Cl). The first step in the Deacon mechanism is the hydrogen abstraction from HCl leading to adsorbed activated chlorine and hydroxyl species (*21*). Then, Hg^0 can be quickly oxidized by the activated chlorine. The series reactions in the presence of Mo−Mn complex can be speculated as follows, in which eq 12 can be regarded as the overall Deacon reaction (*21*). The effect of

Mo^{6+} to the catalysis might be attributed to its promotion on the cycle between Mn^{3+} and Mn^{4+}, which would speed the transfer of oxygen and the formation of the reactive chlorine species (eqs 3−8).

$$Mn^{4+} + O^{2-} + HCl \rightarrow Mn^{3+} + OH^{-*} + Cl^* \quad (3)$$

$$OH^{-*} + OH^{-*} \rightarrow H_2O + O^{2-} \quad (4)$$

$$Cl^* + Cl^* \rightarrow Cl_2 \quad (5)$$

$$2Mn^{3+} + 0.5O_2 \rightarrow 2Mn^{4+} + O^{2-} \quad (6)$$

$$Mo^{6+} + Mn^{3+} \rightarrow Mn^{4+} + Mo^{5+} \quad (7)$$

$$2Mo^{5+} + 0.5O_2 \rightarrow 2Mo^{6+} + O^{2-} \quad (8)$$

$$Hg^0 + Cl^* \rightarrow HgCl^* \quad (9)$$

$$HgCl^* + HCl \rightarrow HgCl_2 + H \quad (10)$$

$$Hg^0 + Cl_2 \rightarrow HgCl_2 \quad (11)$$

$$Hg^0 + 2HCl + 0.5O_2 \xrightarrow{Mo-MnO_x} HgCl_2 + H_2O \quad (12)$$

In conclusion, the Mo doped catalyst $Mn/\alpha\text{-}Al_2O_3$ displayed excellent performance for Hg^0 catalytic conversion. The apparent catalytic reaction rate constant increased by about 5.5 times in the presence of SO_2 at 423 K. The doping of Mo into the catalysts might improve the dispersion of MnO_x particles and form more stable compound that have stronger sulfur-tolerance. The Mo doped catalysts appear to have potential for Hg^0 oxidation from coal fired flue gas in industrial applications.

Acknowledgments

This study was supported by the High-Tech R&D Program of China (863) under Grant No.2007AA06Z340.

Literature Cited

(1) *Global Mercury Assessment, UNEP Chemicals*; United Nations Environment Programme (UNEP): Geneva, Switzerland, December, 2002).
(2) Pavlish, J. H.; Sondreal, E. A.; Mann, M. D.; Olson, E. S.; Galbreath, K. C.; Laudal, D. L.; Benson, S. A. State Review of Mercury Control Options for coal-fired power plants. *Fuel Process. Technol.* **2003**, *82*, 89–165.
(3) United Nations Environment Programme (UNEP), United States Proposes Decision on Mercury at 25 GC/GMEF. http://www.unep.org/pdf/Draft_decision-approved.pdf (accessed Feb 20, 2009).
(4) Wu, Y.; Wang, S. X.; Streets, D. G.; Hao, J. M.; Chan, M.; Jiang, J. K. Trends in anthropogenic mercury emissions in China from 1995 to 2003. *Environ. Sci. Technol.* **2006**, *40*, 5312–5318.
(5) Streets, D. G.; Zhang, Q.; Wu, Y. Projections of global mercury emissions in 2050. *Environ. Sci. Technol.* **2009**, *43*, 2983–2988.
(6) Jiang, G. B.; Shi, J. B.; Feng, X. B. Mercury pollution in China. *Environ. Sci. Technol.* **2006**, *40*, 3672–3678.
(7) Cao, Y.; Gao, Z. Y.; Zhu, J. S.; Wu, Q. H.; Huang, Y. J.; Chiu, C. C.; Parker, B.; Chu, P.; Pan, W. P. Impacts of halogen additions on mercury oxidation, in a slipstream selective catalyst reduction (SCR), reactor when burning sub-bituminous coal. *Environ. Sci. Technol.* **2008**, *42*, 256–261.
(8) Liu, S. H.; Yan, N. Q.; Liu, Z. R.; Qu, Z.; Wang, H. P.; Chang, S. G.; Miller, C. Using bromine gas to enhance mercury removal from flue gas of coal-fired power plants. *Environ. Sci. Technol.* **2007**, *41*, 1405–1412.
(9) Wu, Z. B.; Jiang, B. Q.; Liu, Y. Effect of transition metals addition on the catalyst of manganese/titania for low-temperature selective catalytic reduction of nitric oxide with ammonia. *Appl. Catal., B* **2008**, *79*, 347–355.
(10) Ji, L.; Sreekanth, P. M.; Smirniotis, P. G.; Thiel, S. W.; Pinto, N. G. Manganese oxide/titania materials for removal of NO_x and elemental mercury from flue gas. *Energy Fuels.* **2008**, *22*, 2299–2306.
(11) Qiao, S. H.; Chen, J.; Li, J. F.; Qu, Z.; Liu, P.; Yan, N. Q.; Jia, J. Q. Adsorption and catalytic oxidation of gaseous elemental mercury in flue gas over MnO_x/alumina. *Ind. Eng. Chem. Res.* **2009**, *48*, 3317–3322.
(12) Presto, A. A.; Granite, E. J. Survey of catalysts for oxidation of mercury in flue gas. *Environ. Sci. Technol.* **2006**, *40*, 5601–5609.
(13) Hrdlicka, J. A.; Seames, W. S.; Mann, M. D.; Muggli, D. S.; Horabik, C. A. Mercury oxidation in flue gas using gold and palladium catalysts on fabric filters. *Environ. Sci. Technol.* **2008**, *42*, 6677–6682.
(14) Zhuang, Y.; Laumb, J.; Liggett, R.; Holmes, M.; Pavlish, J. Impacts of acid gases on mercury oxidation across SCR catalyst. *Fuel Process. Technol.* **2007**, *88*, 929–934.
(15) Wu, Z. B.; Jiang, B. Q.; Liu, Y.; Wang, H. Q.; Jin, R. B. DRIFT study of manganese/titania -based catalysts for low-temperature selective catalytic reduction of NO with NH_3. *Environ. Sci. Technol.* **2007**, *41*, 5812–5817.
(16) Kamata, H.; Ueno, S.; Naito, T.; Yukimura, A. Mercury oxidation over the $V_2O_5(WO_3)/TiO_2$ commercial SCR catalyst. *Ind. Eng. Chem. Res.* **2008**, *47*, 8136–8141.
(17) Tikhomirov, K.; Krócher, O.; Elsener, M.; Widmer, M.; Wokaun, A. Manganese based materials for diesel exhaust SO_2 traps. *Appl. Catal., B* **2006**, *67*, 160–167.
(18) Zosimova, A. P.; Smirnov, A. V.; Nesterenko, S. N.; Yuschenko, V. V.; Sinkler, W.; Kocal, J.; Holmgren, H.; Ivanova, I. I. Synthesis, characterization, and sulfur tolerance of Pt-MoO_x catalysts prepared from Pt-Mo alloy precursors. *J. Phys. Chem. C.* **2007**, *111*, 14790–14798.
(19) Infantes-Molina, A.; Mérida-Robles, J.; Rodríguez-Castellón, E.; Fierro, J. L. G.; Jiménez-López, A. Effect of Molybdenum and Tungsten on Co/MSN as Hydrogenation Catalysts. *J Catal.* **2006**, *240*, 258–267.
(20) Wang, C. C.; Weng, H. S. Promoting effect of molybdenum on CuO/gamma-Al_2O_3 catalyst for the oxidative decomposition of $(CH_3)_2S_2$. *Appl. Catal., A* **1998**, *170*, 73–80.
(21) López, N.; Gómez-Segura, J.; Marín, R. P.; Pérez-Ramírez, J. Mechanism of HCl Oxidation (Deacon process) over RuO_2. *J. Catal.* **2008**, *255*, 29–39.
(22) Benson, S. W. *The Foundation of Chemical Kinetics*; McGraw-Hill: New York, 1960.

ES9021206